Novelties in MR Fingerprinting

Gregor Körzdörfer

Siemens Healthineers, Erlangen, Germany

Magnetic Resonance Fingerprinting in brief

Magnetic Resonance Fingerprinting (MRF)[1] is a fast and precise technique for multiparametric quantitative MRI [1]. With MRF several tissue properties can be identified simultaneously in a single acquisition. Sequence parameters are varied pseudorandomly throughout the acquisition, to generate distinguishable tissue signals. These measured signals are then compared with a dictionary of pre-simulated signals. Each signal is unique and can therefore be considered a fingerprint for certain tissue properties. Comparing a measured fingerprint with all dictionary entries allows the most similar simulated fingerprint to be identified, revealing the fingerprint's properties.

Since its first publication in 2013, MRF has sparked much research interest. Besides clinical research with MRF, which is now facilitated by a commercially available implementation, a variety of technical aspects of the concept and extensions have been explored. While a commercially available MR Fingerprinting version requires a high-performance integration on the scanner as well as thorough validation to be ready for use in clinical studies, it should be clear that MR Fingerprinting continues to evolve vividly in the research arena. This includes modifying the acquisition scheme, for example with different *k*-space trajectories and extending the MRF concept to provide additional information such as magnetization transfer [2], diffusion [3], susceptibility and B0 [4] and B1+ [5, 6]. Another research area is optimal sequence design for specific MRF implementations, which can be addressed with optimization algorithms [7, 8].

This article sheds light on some novel developments driven by Siemens Healthineers. Please refer to the referenced literature for further reading.

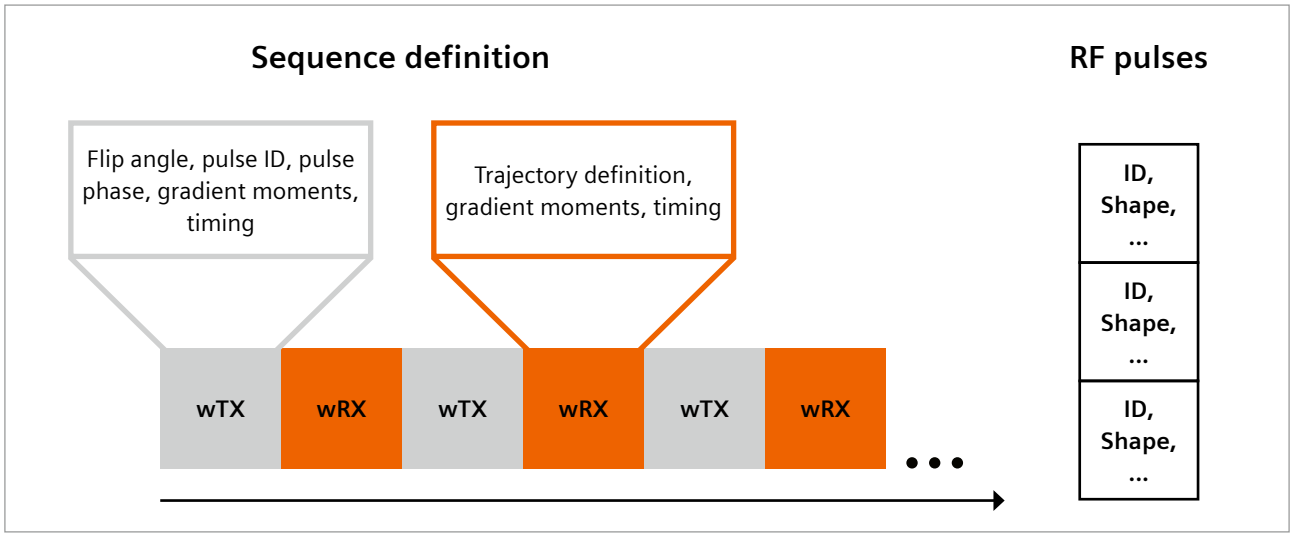

1 A sequence definition and a list of RF pulses labeled with a unique ID. The sequence definition consists of an arbitrary series of warp&TX events (wTX) and warp&RX events (wRX). In each wTX block the gradient moments and timing before the RF pulse are recorded, as is the specified RF pulse ID (linked from the RF pulse list) with its prescribed flip angle and phase. The wRX block contains information on the gradient moments and timing before the signal is sampled and the echo sampling time. Trajectory information can be contained or defined later at the scanner.

[1] *The product/feature (mentioned herein) is not commercially available in some countries. Due to regulatory reasons its future availability cannot be guaranteed.*

Promoting research: MRF development kit

One strength of the MRF idea is the freedom to combine different sequences and sampling schemes to optimize and extend MRF. However, quantitative MRI in general requires carefully considered sequence design and attention to detail, as it is highly sensitive to deviations between real experiment and limited theoretical models. Common effects are deviations in sampling trajectory, inhomogeneities of B0 and B1+, and effects not included in the signal model in general. Much effort needs to be spent in programming sequences, performing simulations for the dictionary, and implementing reconstruction algorithms and further infrastructure to handle the large amount of data, using performant data structures and interfaces. Some specific pitfalls are:

- The sequence scheme is replicated offline for the dictionary simulation and so may deviate from the actual scheme played out on the scanner in small but crucial details, such as RF-pulse profiles or the exact gradient moments. This of course also applies to conventional mappings where a simplistic signal model may not reflect the physical reality.
- A variety of Bloch simulators or extended phase graph algorithms exist that may lead to varying results for the same sequence input. These can be arbitrarily parametrized, which might further alter results between different handcrafted simulators.
- Once there is more than a single MRF version employed, special provisions are required to safely link each measured raw data file to the corresponding dictionary file. The same applies to changes of sequence parameters "on the fly", which may render the designated dictionary invalid. Reconstructions with a wrong dictionary will result in wrong mapping results, and the error may be hard to detect, so this must be avoided.

To simplify and harmonize the development of novel MRF implementations, we provide a framework that elegantly solves the aforementioned problems. This framework provides data structures for describing an MR sequence in a generic way.

A sequence is described by a chain of warp&TX (wTX) and warp&RX (wRX) blocks (Fig. 1). A wTX block consists of the gradient moments before a transmit pulse, as well as the gradient during the pulse, and the pulse ID. RF pulses can be stored in a different data structure, so that the same RF pulse can be used in multiple wTX events (Fig. 1). The wRX events contain similar gradient moment information, and also information about when signals are to be sampled. Blocks can contain trajectory information, but generally do not need to, because the assumption underlying today's MRF approaches is that simulated fingerprints are independent of in-plane pixel position – so trajectory information is usually not important for signal generation or for simulation, and it can be defined later directly at the scanner.

This sequence definition can be represented by a simple data structure, which can be easily filled using different programming languages such as Python, C++ and MATLAB. Together with a definable set of tissues, and ranges for physical parameters such as T1, T2, and B1+, it is then handed over to a fast C++ standalone Bloch simulator that rapidly creates a dictionary.

Both the sequence definition and dictionary are then wrapped together into an MRF container (Fig. 2). This container can be run on the scanner using an interpreter that executes the sequence definition. Acquired data is reconstructed in the ICE (Image Calculation Environment) environment utilizing the dictionary stored in the container, and finally DICOM images are generated.

The package facilitates the development of new MRF applications, and especially their direct application in

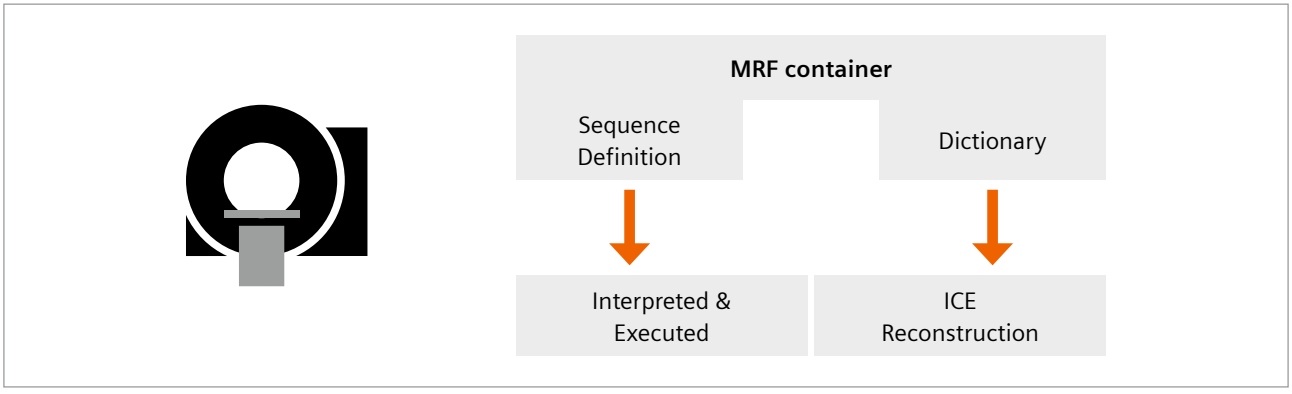

2 An MRF container with sequence definition and corresponding dictionary can be loaded onto the scanner. The sequence definition is interpreted and executed, and then tissue parameters are reconstructed using the dictionary for this sequence directly in ICE, generating DICOM maps.

clinical studies, due to its full scanner integration. Users also benefit from other features such as integrated correction methods for non-Cartesian sampling trajectories, and advanced reconstruction methods described later in this article.

One convenient and beginner-friendly application is parametrizing a spiral FISP MRF [9] sequence (Fig. 3). The user can specify repetition times, flip angles and phases of the pulses, as well as the parameters T1, T2, and B1+. A C++ standalone program then writes a FISP MRF sequence definition and dictionary files, which can be simply copied to the scanner for execution.

3D MRF

The framework idea also applies to 3D sequences. 3D acquisitions provide significant speedup and improved resolution for MRF. In addition to higher signal to noise ratio (SNR), a potentially more efficient undersampling along all three spatial dimensions can be employed. Examples are 3D Cartesian [10] or spiral projection sampling schemes. A 3D spiral stack FISP MRF sequence has recently been successfully applied in clinical studies for detecting epileptic lesions [11] and hippocampal sclerosis [12].

Novel reconstruction methods for MRF

MRF estimates parameter maps from highly undersampled signals. Assuming that spatial undersampling artifacts can be treated as noise in the temporal signal domain, dictionary matching can even be performed without any further measures. However, more advanced techniques aim to reconstruct better quality parameter maps by taking the effect of undersampling into account. An example is CS-MRF [13] which is an iterative gradient proximal algorithm for MRF, that uses the concepts of compressed sensing. An estimated image series is calculated in three steps: a gradient step to enforce data consistency; fingerprint dictionary matching; and spatial regularization via total variation regularization. CS-MRF extends the iterative reconstruction algorithm AIR MRF [14] with this spatial regularization. This provides parameter maps free of undersampling artifacts, as well as maps with lower noise, while fine structures and boundaries between tissues are preserved. Figure 4 shows an example of a volunteer's brain acquired at 3 mm slice thickness (acquisition time per slice: 21 seconds at 1 mm in-plane resolution) reconstructed with and without CS-MRF. Especially fine details are better visible, and the overall image impression is better with CS-MRF due to reduced noise.

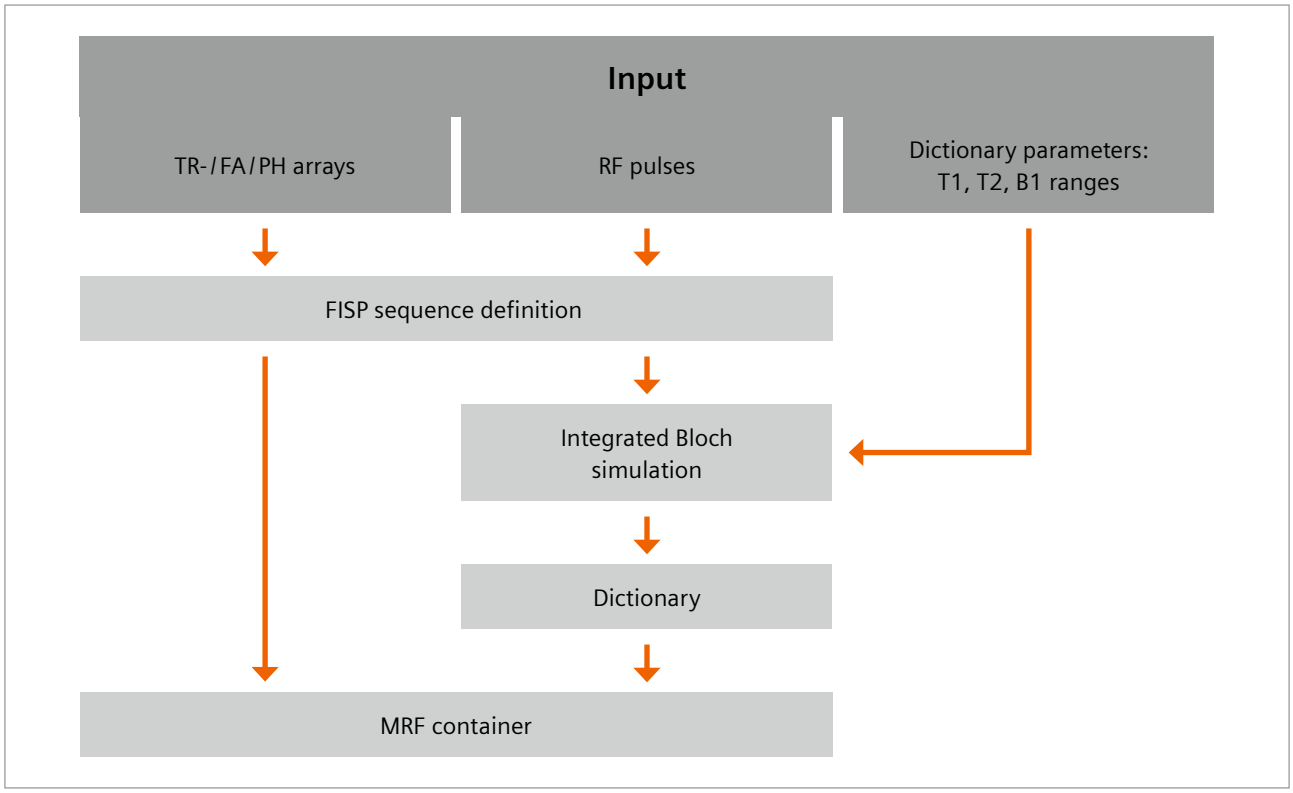

3 Example of a user-friendly use case for the MRF development kit. The user defines repetition time (TR), flip angle (FA) and pulse phase (PH) arrays, RF pulses, and the dictionary parameter ranges for T1, T2, and B1. With this information a precompiled program writes a spiral FISP MRF sequence definition, calculates the matching dictionary, and packs both together into an MRF container.

Another challenge for MRF reconstructions is the high computational effort, in particular if the dictionary increases in size. Every measured signal must be compared with every dictionary entry. Since every dictionary can only have a finite number of entries, the resulting maps are limited to this discrete set of entries, and are therefore intrinsically inaccurate. Furthermore, the more entries the dictionary contains, the more reconstruction time is required. Deep learning (DL) can be used to provide continuous parameter estimations, accelerate the MRF reconstruction process, and eliminate the burden of high storage requirements during the reconstruction. Reconstruction with DL algorithm is performed by passing the signal (or a set of signals from e.g., neighboring voxels) through a network, which predicts the T1 and T2 relaxation times from the input. Proposed approaches include fully connected neural networks (FCNs) and convolutional neural networks (CNNs). However, even state-of-the-art DL algorithms have their drawbacks. FCNs tend to overfit because of the huge number of optimizable parameters. CNNs are not optimally suited for time-resolved tasks.

To overcome these limitations, we recently evaluated recurrent neural networks (RNNs) due to their ability to better capture the continuous time dependency in typical MRF signals [15, 16]. RNNs (Fig. 5) were evaluated on *in vivo* data from several volunteers' brains. The results show that with this approach, precise parameter maps can be reconstructed in an extremely short time. RNNs are especially promising for large dictionaries comprising multiple dimensions, where conventional matching algorithms are limited due to the exponential character of the problem. Another promising approach is to separate the DL reconstruction into two networks: a first artifact reduction network cleans and restores the input signals, which are then fed into the regression network [17].

Motion detection for MRF

Motion artifacts in MRI are usually accompanied by visible image artifacts. In quantitative MRI, results may be affected in a more subtle way: values in the parametric maps can be corrupted without obvious hints in the appearance of the maps. MRF has a certain inherent robustness regarding motion due to the applied pattern matching approach. However, while MRF is indeed fairly insensitive to in-plane motion (as excited signal remains in the imaging plane), several works suggest that 2D FISP MRF is more sensitive to strong through-plane motion (as new spins enter the imaging plane during the acquisition).

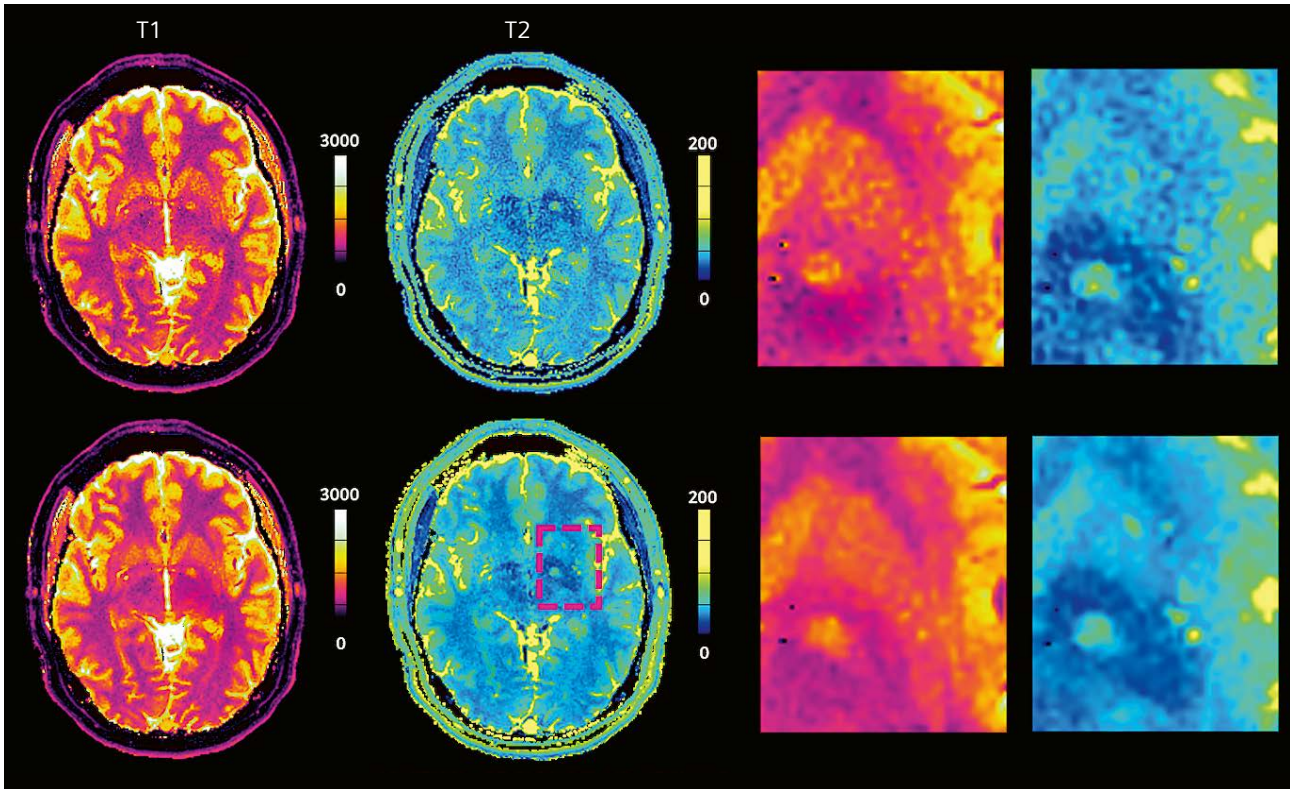

4 Top row: conventionally reconstructed FISP MRF T1 (first column) and T2 (second column) maps (21 seconds acquisition time per slice, slice thickness 3 mm, in-plane resolution 1 mm) with a zoomed excerpt on the right. Bottom row: The same slice parameter maps reconstructed using CS-AIR have substantially less noise while image details and tissue boundaries are preserved as observable in the excerpt on the right.

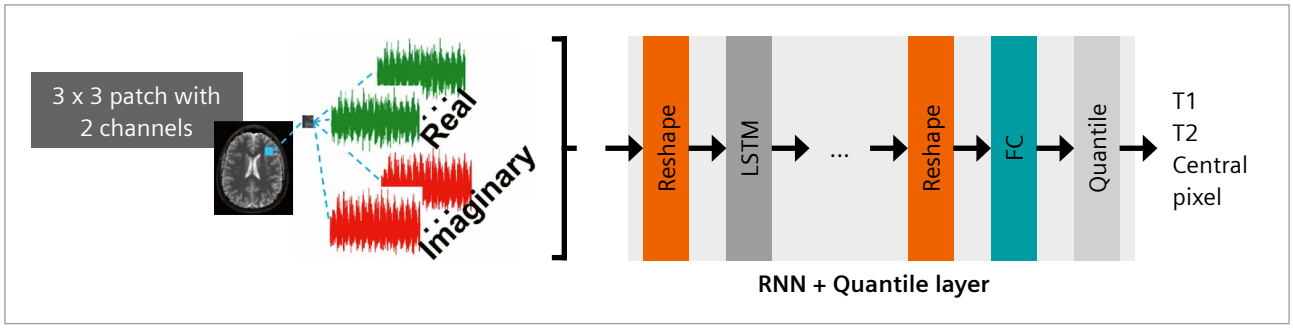

5 Architecture of the neural network for quantifying T1 and T2 from signals in MRF. A patch of complex signals is used as input and fed through a recurrent neural network (RNN) plus a quantile layer. (LSTM: long-short-term memory layer, FC: fully connected layer)

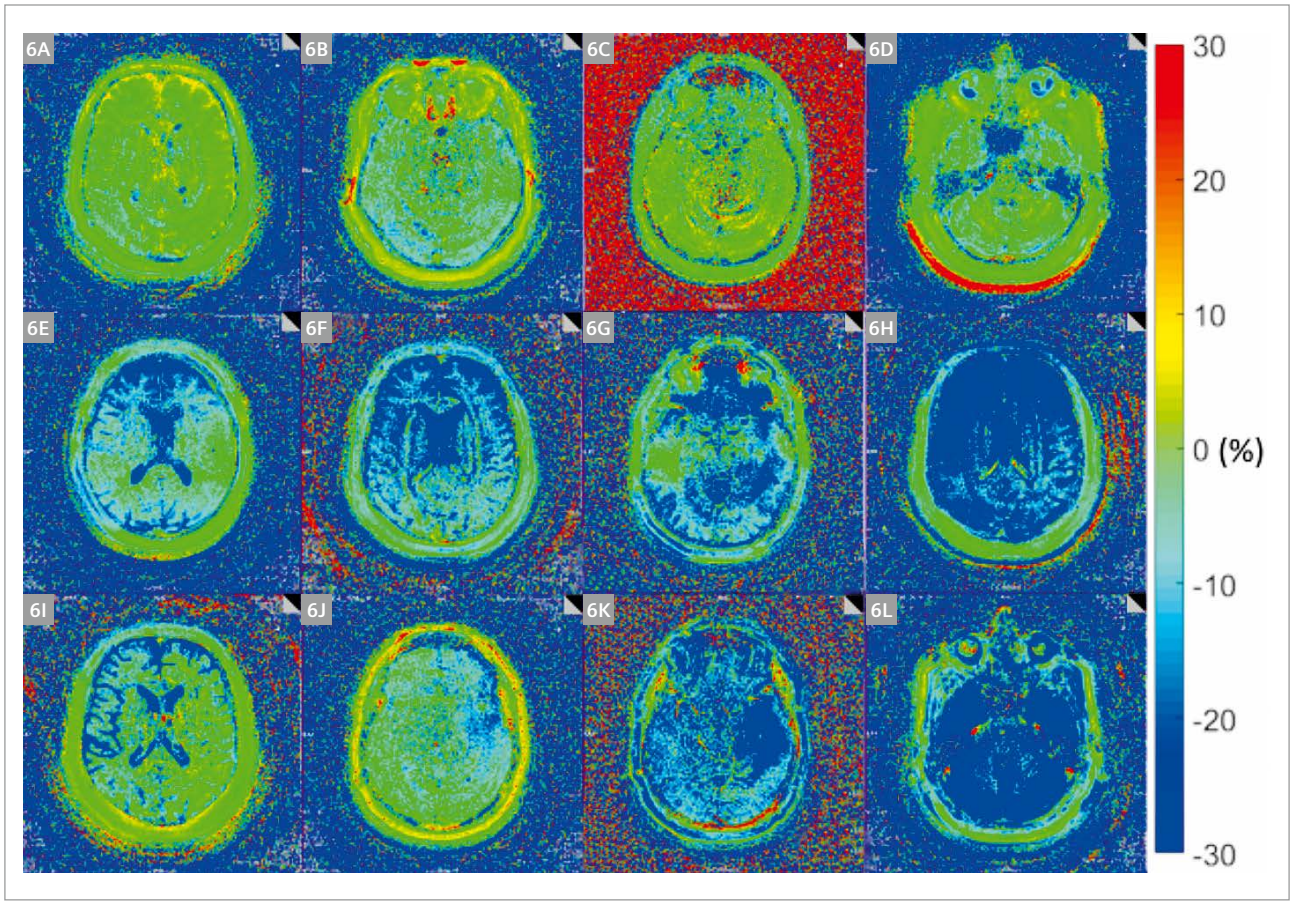

6 Exemplary residual maps (rel. deviation in %) obtained from patient brain MRF scans. 6A–D show residual maps where no motion occurred. 6E shows a pattern that corresponds to slight nodding; 6F and G medium nodding; 6H strong nodding. 6I and J show tilting of the head. 6K shows a slight stretching movement, and 6L a strong one.

Consequently, there should be a way to at least detect the presence of motion-related errors. A prototype method [18] demonstrates that this is feasible without any additional navigator scans or camera devices. It relies on the fact that bulk movement of the head is rigid (flowing CSF is not considered), and that signal alterations due to motion have high frequency compared with dictionary signals. The concept consists in comparing measured signals with the corresponding matched dictionary signals at different timepoints. This is possible due to the high sampling rate of spiral FISP MRF [9], where approximately every 600 microseconds a fully sampled image can be reconstructed from a set of single spiral frames.

These images do not provide a well-defined contrast, as the signal in MRF also varies strongly on short time scales, but they do enable the calculation of spatially and temporally resolved residuals with respect to the predicted ideal signal from the dictionary. These residuals exhibit certain patterns characteristic of typical head movements such as nodding, tilting, and stretching. Examples are shown in Figure 6. These can be evaluated manually or automatically, using a fitting algorithm such as a neural network. By doing a weighted sum of all detected motion patterns, an overall estimate (non, low, medium, strong) of the motion effect in a slice can be determined.

The technique was evaluated in volunteers and 32 patients with suspicion of glioma. Two MRF acquisitions were performed, so the difference between the two acquisitions could be related to the detected motion. Where there was no detected motion, the average difference of parameter values from the two acquisitions was approximately 2%. For acquisition pairs where one was not motion corrupted and the other exhibited low, medium, or strong motion, the average differences were 3%, 5% and 25% respectively. With the help of the algorithm, motion corrupted scans could be identified reliably. Overall in 77% of all measured slices no motion, in 8.8% low motion, in 9.4% medium motion, and in 4.8% strong motion was detected.

References

1 D. Ma, V. Gulani, N. Seiberlich, K. Liu, J. L. Sunshine, J. L. Duerk, and M. A. Griswold, "Magnetic resonance fingerprinting," Nature, vol. 495, no. 7440, pp. 187–192, 2013.

2 Hilbert, T, Xia, D, Block, KT, et al. Magnetization transfer in magnetic resonance fingerprinting. Magn Reson Med. 2019; 00: 1–14.

3 Jiang, Yun, et al. "Simultaneous T1, T2 and Diffusion Quantification using Multiple Contrast Prepared Magnetic Resonance Fingerprinting." Proceedings of the 25th Annual Meeting of ISMRM, Honolulu, HI, USA. 2017.

4 Körzdörfer, G, Jiang, Y, Speier, P, et al. Magnetic resonance field fingerprinting. Magn Reson Med. 2019; 81: 2347–2359.

5 Cloos, M., Knoll, F., Zhao, T. et al. Multiparametric imaging with heterogeneous radiofrequency fields. Nat Commun 7, 12445 (2016).

6 Buonincontri, G. and Sawiak, S.J. (2016), MR fingerprinting with simultaneous B1 estimation. Magn. Reson. Med., 76: 1127–1135.

7 Zhao, Bo, et al. "Optimal Experiment Design for Magnetic Resonance Fingerprinting: Cramer-Rao Bound ´Meets Spin Dynamics" in IEEE Transactions on Medical Imaging, vol. 38, no. 3, pp. 844–861, 2019.

8 Cohen, Ouri, et al. "Algorithm comparison for schedule optimization in MR fingerprinting" in Magnetic Resonance Imaging, vol. 41, pp. 15–21, 2017.

9 Y. Jiang, D. Ma, N. Seiberlich, V. Gulani, and M. A. Griswold, "MR fingerprinting using fast imaging with steady state precession (FISP) with spiral readout," Magnetic resonance in medicine, vol. 74, no. 6, pp. 1621–1631, 2015.

10 Jiang, Yun, et al. "Fast 3D MR Fingerprinting with Pseudorandom Cartesian Sampling." Proceedings of the 27th Annual Meeting of ISMRM, Montréal, Canada. 2019.

11 Ma, D., Jones, S.E., Deshmane, A., Sakaie, K., Pierre, E.Y., Larvie, M., McGivney, D., Blümcke, I., Krishnan, B., Lowe, M., Gulani, V., Najm, I., Griswold, M.A. and Wang, Z.I., "Development of high-resolution 3D MR fingerprinting for detection and characterization of epileptic lesions". J. Magn. Reson. Imaging, 49: 1333–1346, 2019

12 Congyu Liao, Kang Wang, Xiaozhi Cao, Yueping Li, Dengchang Wu, Huihui Ye, Qiuping Ding, Hongjian He, and Jianhui Zhong, "Detection of Lesions in Mesial Temporal Lobe Epilepsy by Using MR Fingerprinting", Radiology 2018 288:3, 804–812.

13 S. Arberet, X. Chen, B. Mailhé, P. Speier, and M. S. Nadar, "CS-MRF: Sparse & low-rank iterative reconstruction for magnetic resonance fingerprinting" in ISMRM Workshop on Magnetic Resonance Fingerprinting, 2017.

14 Christopher C. Cline, Xiao Chen, Boris Mailhe, Qiu Wang, Josef Pfeuffer, Mathias Nittka, Mark A. Griswold, Peter Speier, Mariappan S. Nadar, AIR-MRF: Accelerated iterative reconstruction for magnetic resonance fingerprinting, Magnetic Resonance Imaging, 74: 29–40, 2017.

15 Hoppe, Elisabeth, et al. "Deep learning for magnetic resonance fingerprinting: Accelerating the reconstruction of quantitative relaxation maps." Proceedings of the 26th Annual Meeting of ISMRM, Paris, France. 2018.

16 Hoppe, Elisabeth, et al. "RinQ Fingerprinting: Recurrence-Informed Quantile Networks for Magnetic Resonance Fingerprinting." International Conference on Medical Image Computing and Computer-Assisted Intervention. Springer, Cham, 2019.

17 Xu, Yiling, et al. "Learning how to Clean Fingerprints – Deep Learning based Separated Artefact Reduction and Regression for MR Fingerprinting." Proceedings of the 28th Annual Meeting of ISMRM, Paris, France. 2020.

18 Körzdörfer, Gregor, et al. "Data-driven Motion Detection for MR Fingerprinting" Proceedings of the 28th Annual Meeting of ISMRM, Paris, France. 2020.

Contact

Gregor Körzdörfer
Siemens Healthineers
SHS DI MR DL Orth
Erlangen, Germany
Tel.: +49 (0) 9131 84-7192
Gregor.Koerzdoerfer@siemens-healthineers.com